

LETTER TO THE EDITOR



Retractosomes: small extracellular vesicles generated from broken-off retraction fibers

© CEMCS, CAS 2022

Cell Research (2022) 32:953–956; <https://doi.org/10.1038/s41422-022-00666-2>

Dear Editor,

Various cell protrusions are known to generate extracellular vesicles.¹ A migratory cell generates retraction fibers (RFs) and migrasomes during migration. After the cell migrates away, large amounts of RFs break off from the cell and are left behind. The fate of RFs after detaching from cells is currently unknown.² To investigate the fate of RFs, we observed Tspan4-overexpressing L929 cells with live-cell imaging (Supplementary information, Data S1). We found that during migration, RFs are pulled out at the trailing edge of cells, and migrasomes soon form on the tips or branch points of the RFs. At this stage, the Tspan4 signal is evenly distributed along the RFs (Fig. 1a). Eventually, the RFs start to break. In most cases, the sections of RF far away from the cells break first, which is not surprising, as these sections of RF are formed earlier. Interestingly, after the RFs break up, the Tspan4 signal appears as a large number of small puncta along the paths which were occupied by the RFs (Fig. 1a; Supplementary information, Video S1).

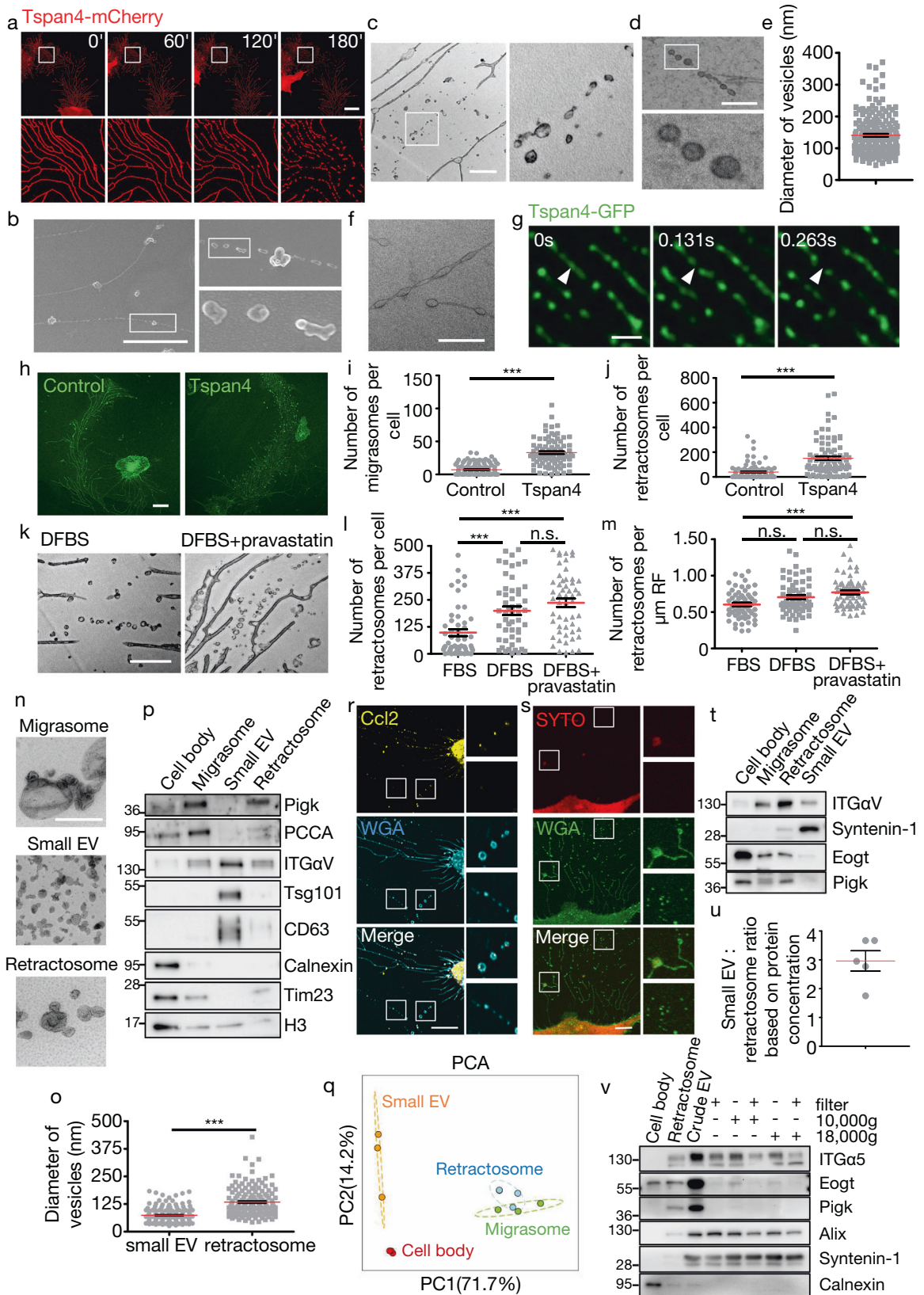
To investigate the morphology of these RF puncta, we carried out scanning electron microscopy (SEM) analysis. On the far end of RFs, large numbers of round, small extracellular vesicles are left behind; in many cases these vesicles are linked together, like a string of beads (Fig. 1b). To check whether these vesicles have a continuous membrane, we carried out transmission electron microscopy (TEM). TEM revealed that these vesicles indeed have a continuous membrane (Fig. 1c), and thus they are true vesicles instead of broken membrane fragments. Cryo-TEM analysis, which can better preserve the morphology of delicate membrane structures, further confirmed that the RF puncta are small extracellular vesicles (Fig. 1d). These vesicles are much smaller than migrasomes, with size varying from 50 nm to 250 nm (Fig. 1e). These data suggest that when RFs break up, they form a type of previously unreported extracellular vesicle. Similar to migrasomes, these small extracellular vesicles are migration-dependent: treating cells with blebbistatin blocks their formation (Supplementary information, Fig. S1a–c). Thus, we named these vesicles “retractosomes”, to reflect their RF and plasma membrane origin. The beads-on-a-string structure is frequently observed under cryo-TEM (Fig. 1f). This indicates that, before breaking, the RF goes through a stage of morphological transformation, with sections of the RF bulging into small vesicles, which likely form retractosomes. Wheat germ agglutinin (WGA) effectively labels RFs and migrasomes.³ WGA staining revealed that retractosomes are formed by all the migratory cells we tested, none of which ectopically expressed Tspan4 (Supplementary information, Fig. S1d). Moreover, we observed formation of retractosomes in various *in vivo* settings, including circulating neutrophils in mice, and embryonic cells during zebrafish gastrulation (Supplementary information, Fig. S2a, b).

Migrasome formation is driven by assembly of tetraspanin-enriched macrodomains, and overexpression of Tspan4 can markedly enhance migrasome and RF formation.⁴ To test whether tetraspanins are also involved in retractosome formation, we overexpressed Tspan4-GFP in L929 cells. Similar to migrasomes, Tspan4-GFP is enriched in retractosomes. Live-cell imaging using resonant scanning mode reveals that Tspan4 starts to condense and becomes enriched in puncta along the RF before the RF breaks; these puncta eventually become retractosomes (Fig. 1g). Moreover, we found that overexpression of Tspan4 significantly enhances both migrasome and retractosome formation (Fig. 1h–j). This effect on retractosomes is largely due to enhanced RF formation. In Tspan4-overexpressing cells, RFs show a 2.68-fold increase in the total length, which then break into more retractosomes (Supplementary information, Fig. S1e).

Migrasomes are formed by assembly of cholesterol- and tetraspanin-enriched macrodomains.⁴ The condensation of the Tspan4 signal along the RF before transformation into retractosomes prompted us to check whether retractosomes are formed by the same mechanism. First, we checked whether cholesterol is enriched on retractosomes. We found that cholesterol is hardly detected on retractosomes (Supplementary information, Fig. S3a). Detailed analysis showed that cholesterol is much less enriched on retractosomes than on migrasomes (Supplementary information, Fig. S3b). This suggests that retractosomes may form by mechanisms other than assembly of tetraspanin-enriched macrodomains.

To directly test this hypothesis, we cultured cells in cholesterol depletion medium and then checked the retractosome formation. As we reported earlier, depletion of cholesterol blocks migrasome formation; in contrast, cholesterol depletion promotes retractosome formation (Fig. 1k–m; Supplementary information, Fig. S3c, d). Taken together, these data suggest that retractosome formation depends on Tspan4 but not cholesterol, which is different from migrasome formation.

Next, we studied the protein composition of retractosomes. To isolate retractosomes, we first removed the culture medium and washed the cells with PBS, which removes the majority of small extracellular vesicles (EVs). Next, we collected the cells and performed two steps of low-speed centrifugation to remove cell bodies and large debris. We removed migrasomes by passing the sample through a 0.22- μ m filter. Finally, to collect retractosomes, we subjected the flow-through to high-speed centrifugation (Supplementary information, Fig. S4a).⁵ Although this isolation protocol yields a mixture of retractosomes and broken-off RFs, the retractosomes are generated by broken-off RFs, and thus the protein composition of this sample should be largely the same as the protein composition of retractosomes. The sample was checked by electron microscopy, which revealed vesicles with sizes ranging from 50 nm to 250 nm (Fig. 1o). The morphology



and size of the isolated retractorosomes are very similar to those of retractorosomes in cultured cells. The isolated retractorosomes are smaller than migrasomes but slightly larger than small EVs (Fig. 1n, o). To further check the purity of retractorosomes, we carried out

western blot analysis using antibodies against various markers of migrasomes and small EVs (Fig. 1p; Supplementary information, Fig. S5). We found that the isolated retractorosomes contain very low levels of Tsg101, CD63 and Syntenin-1 proteins, three

Fig. 1 Retraction fibers can break into small vesicles. **a** Breakage of RFs. Tspan4-mCherry-expressing L929 cells were cultured for 6 h, and time-lapse images were acquired at 7.5 min per frame with an Olympus FV3000 confocal microscope. Scale bar, 10 μ m. **b** SEM analysis of L929 cells expressing Tspan4-GFP. Tspan4-GFP-expressing L929 cells were grown on a 35-mm confocal chamber for 12 h and observed by field emission SEM. The boxed area in the main image is enlarged at top right. The boxed area in the top right panel is enlarged at bottom right. Scale bar, 10 μ m. **c** TEM analysis of L929 cells expressing Tspan4-GFP. TEM image (left) and enlarged image (right) of an ultra-thin section of a Tspan4-GFP-expressing L929 cell cultured on a 35-mm confocal chamber for 12 h. Scale bar, 500 nm. **d** Cryo-TEM analysis of L929 cells expressing Tspan4-GFP. Cells were cultured on a 3-mm sapphire disc, then fixed by high pressure freezing. Freeze substitution was started at -90°C and the samples were slowly warmed to 0°C with 2% osmium tetroxide in acetone. The samples were washed with acetone, then infiltrated and embedded in SPI-Pon 812 Resin. 70-nm sections were checked under TEM. Scale bar, 1 μ m. **e** Retractsomes from analysis shown in **c** were quantified for the diameter. Data shown represent means \pm SEM. $n = 150$ retractsomes from three independent experiments. **f** Cryo-TEM analysis of the “beads-on-a-string” structure. Wild-type L929 cells were cultured on a 3-mm sapphire disc, then fixed by high pressure freezing. Freeze substitution was started at -90°C and the samples were slowly warmed to 0°C with 2% osmium tetroxide in acetone. The samples were washed with acetone, then infiltrated and embedded in SPI-Pon 812 Resin. 70-nm sections were checked under TEM. Scale bar, 1 μ m. **g** Time-lapse images of RFs of a Tspan4-GFP-expressing cell obtained in resonant scanning mode. The arrowhead indicates breaking of a RF to form a retractsome. Scale bar, 1 μ m. **h** Representative image of wild-type and Tspan4-mCherry-expressing L929 cells dyed with WGA488. Cells were cultured for 18 h, dyed with WGA488 and imaged with an Olympus FV3000 confocal microscope. Scale bar, 10 μ m. **i** Cells from analysis shown in **h** were quantified for the number of migrasomes per cell. Data shown represent means \pm SEM. $n = 66$ cells from three independent experiments. Two-tailed unpaired *t*-test was used. $***P < 0.001$. **j** Cells from analysis shown in **h** were quantified for the number of retractsomes per cell. Data shown represent means \pm SEM. $n = 66$ cells from three independent experiments. Two-tailed unpaired *t*-test was used. $***P < 0.001$. **k** TEM image of an ultra-thin section of a Tspan4-GFP-expressing L929 cell cultured on a 35-mm confocal chamber in cholesterol depletion medium (DFBS) with or without treatment of $30\ \mu\text{M}$ pravastatin for 12 h. Scale bar, 1 μ m. **l** Tspan4-GFP-expressing L929 cells were cultured in control medium or cholesterol depletion medium with or without treatment of $30\ \mu\text{M}$ pravastatin for 12 h, and images were acquired with an Olympus FV3000 confocal microscope. The number of retractsomes per cell was quantified. Data shown represent means \pm SEM. $n = 70$ cells from three independent experiments. Two-tailed unpaired *t*-tests were used. $***P < 0.001$; n.s., not significant. **m** Cells from assay shown in **l** were quantified for the number of retractsomes per μ m RF. Data shown represent means \pm SEM. $n = 70$ cells from three independent experiments. Two-tailed unpaired *t*-tests were used. $***P < 0.001$; n.s., not significant. **n** Typical negative staining EM images of purified small EVs, migrasomes and retractsomes. Scale bar, 0.5 μ m. **o** Purified small EVs and retractsomes from **n** were quantified for diameter. Data shown represent means \pm SEM. $n = 150$ small EVs or retractsomes from three independent experiments. Two-tailed unpaired *t*-tests were used. $***P < 0.001$. **p** Samples of cell bodies, purified migrasomes, small EVs and retractsomes from D2SC cells were analyzed by western blotting using antibodies against the identified migrasome-specific markers Pigk and PCCA; the plasma membrane marker ITG α V; the small EV markers Tsg101 and CD63; the ER marker calnexin; the mitochondrion marker Tim23; and the nuclear marker H3. **q** Principal components analysis of the protein composition of cell bodies, migrasomes, small EVs and retractsomes from D2SC cells. **r** Immunostaining of endogenous Ccl2 in D2SC cells. The enlarged images on the right show migrasomes (top) and retractsomes (bottom). Scale bar, 10 μ m. **s** Representative image of an L929 cell stained with WGA488 and SYTO14. The enlarged images on the right show migrasomes (top) and retractsomes (bottom). Scale bar, 10 μ m. **t** Quality control western blot of purified migrasomes, retractsomes and small EVs for analysis shown in **u**. Eogt is marker for migrasome. **u** Ratio of small EVs to retractsomes based on total protein amount. Data shown represent means \pm SEM from five independent experiments. **v** Small EVs purified from culture medium do not contain a significant amount of retractsomes. “Retractsome” indicates retractsomes purified from cultured cells, and “Crude EV” indicates the crude preparation of EVs collected by pelleting the culture medium at $120,000\times g$. Small EVs were isolated from culture medium by treating with or without filtration, and then subjected to $10,000\times g$, $18,000\times g$ or no centrifugation, and finally $120,000\times g$ centrifugation. Samples of cell body and retractsome were loaded with equal protein amount, while samples of retractsome and small EVs isolated with different ways were loaded with equal cell number.

well-established markers for small EVs.⁶ Thus, the isolated retractsomes are not contaminated with significant amounts of small EVs. We found that although the isolated retractsomes contain migrasome markers such as Pigk, Eogt, and PCCA, PCCA and to some extent Eogt, tend to be less enriched in the retractsome fraction compared to the migrasome fraction. Moreover, we found the presence of a small amount of mitochondrial protein Tim23 in the migrasome fraction, which may result from basal level of mitocytosis, a migrasome-dependent mechanism to evict damaged mitochondria,⁷ while Tim23 could not be detected in the retractsome fraction (Fig. 1p; Supplementary information, Fig. S5).

Next, we subjected retractsomes to mass spectrometry analysis. We found that the protein profile of retractsomes is significantly different from that of cell bodies: 1107 proteins were enriched and 1309 proteins were depleted in retractsomes compared to cell bodies (Supplementary information, Fig. S4b). We carried out quantitative mass spectrometry analysis on isolated small EVs and migrasomes. We found that the protein composition of retractsomes shares significant similarity with that of migrasomes, but is very different from that of small EVs (Fig. 1q).

During zebrafish embryonic development, migrasomes modulate organogenesis by enriching and releasing chemokines at spatially restricted locations.⁸ Therefore, we tested whether retractsomes also contain chemokines. For this purpose, we used D2SC cells, a dendritic cell line in which the chemokines Ccl2



and Ccl9 are expressed. We found that both Ccl2 and Ccl9 are enriched in migrasomes; in contrast, some but not all retractsomes contained these chemokines (Fig. 1r; Supplementary Fig. S4c). Recently, we reported that migrasomes contain mRNA and can be stained by SYTO14, a dye for nucleic acids.⁹ In contrast to migrasomes, retractsomes showed no SYTO14 signal (Fig. 1s). Thus, retractsomes have a different cargo composition from migrasomes.

A migrating cell can generate both retractsomes and small EVs. We investigated the relative amount of retractsomes and small EVs generated by the same cultured cells. To do so, we first took the culture medium and used high-speed centrifugation to isolate the crude small EV fraction. We then washed the plate and collected retractsomes as described above. We then diluted the isolated crude small EV and retractsome fractions with an equal volume of buffer and checked the relative amount of small EVs and retractsomes based on the total protein concentration. The purity of the isolated small EVs and retractsomes was checked by western blot (Fig. 1t). Based on total protein concentration, we estimated that the total amount of protein in small EVs is roughly three-fold more than that in retractsomes (Fig. 1u).

So far, various protocols have been used to isolate small EVs. The similar size of retractsomes and small EVs raises the possibility that some of the small EV isolation protocols, especially size-based protocols, may yield a mixed population of retractsomes and small EVs. To test this possibility, we isolated small EVs using various widely used protocols, and then we assessed

retractosome contamination by checking for the presence of migrasome/retractosome markers Eogt and Pigk. As a control, we also checked small EV markers Alix and Syntenin-1. We found that retractosomes did not significantly contaminate the small EV fraction prepared following the widely used protocols (Fig. 1v).

In summary, we describe the discovery of retractosomes, a type of small extracellular vesicle which is generated from broken-off RFs. The physiological functions of retractosomes remain to be determined.

Yizheng Wang^{1,2}, Shuaxin Gao³, Yuheng Liu¹, Dongju Wang¹,
Boqi Liu¹, Dong Jiang¹, Catherine C. L. Wong^{3,4,5,6,7}
Yang Chen^{3,4} and Li Yu¹

¹State Key Laboratory of Membrane Biology, Tsinghua University-Peking University Joint Center for Life Sciences, Beijing Frontier Research Center for Biological Structure, School of Life Sciences, Tsinghua University, Beijing, China. ²Joint Graduate Program of Peking-Tsinghua, National Institute of Biological Sciences, Tsinghua University, Beijing, China. ³Center for Precision Medicine Multi-Omics Research, Peking University Health Science Center, Peking University, Beijing, China. ⁴School of Basic Medical Sciences, Peking University Health Science Center, Beijing, China. ⁵Peking-Tsinghua Center for Life Sciences, Beijing, China. ⁶Peking University First Hospital, Beijing, China. ⁷Advanced Innovation Center for Human Brain Protection, Capital Medical University, Beijing, China.
email: liyulab@mail.tsinghua.edu.cn

REFERENCES

- Rilla, K. J. *Extracell. Vesicles* **10**, <https://doi.org/10.1002/jev2.12148> (2021).
- Ma, L. et al. *Cell Res.* **25**, 24–38 (2015).
- Chen, L., Ma, L. & Yu, L. *Cell Discov.* **5**, <https://doi.org/10.1038/s41421-018-0078-2> (2019).
- Huang, Y. et al. *Nat. Cell Biol.* **21**, 991–1002 (2019).
- Zhao, X. et al. *Cell Discov.* **5**, <https://doi.org/10.1038/s41421-019-0093-y> (2019).
- Thery, C., Amigorena, S., Raposo, G. & Clayton, A. *Curr. Protoc. Cell Biol.* Chapter 3: Unit 3.22 (2006).
- Jiao, H. et al. *Cell* **184**, 2896–2910.e13 (2021).
- Jiang, D. et al. *Nat. Cell Biol.* **21**, 966–977 (2019).
- Zhu, M. et al. *Cell Res.* **31**, 237–240 (2021).

ACKNOWLEDGEMENTS

This research was supported by the Ministry of Science and Technology of China (2017YFA0503404), the National Natural Science Foundation of China (92054301, 31790401, and 32030023), and Beijing Municipal Science & Technology Commission (Z201100005320019). We thank the State Key Laboratory of Membrane Biology, SLSTU-Nikon Biological Imaging Center, Core Facility, Center of Biomedical Analysis, Tsinghua University, for technical support.

AUTHOR CONTRIBUTIONS

L.Y. and Y.W. conceived the experiments. Y.W. and D.W. performed the cell biology and biochemical experiments. S.G. performed the label free quantitative mass spectrum, and Y.L., C.C.L.W. and Y.C. analyzed the mass spectrum data. B.L. and D.J. performed the in vivo experiments. L.Y. supervised the project. L.Y. and Y.W. wrote the manuscript. All authors discussed the manuscript, commented on the project and contributed to manuscript preparation.

COMPETING INTERESTS

The authors declare no competing interests.

ADDITIONAL INFORMATION

Supplementary information The online version contains supplementary material available at <https://doi.org/10.1038/s41422-022-00666-2>.

Correspondence and requests for materials should be addressed to Li Yu.

Reprints and permission information is available at <http://www.nature.com/reprints>